Clay Minerals (2021), **56**, 261–268
doi:10.1180/clm.2022.6

CAMBRIDGE UNIVERSITY PRESS

Article

Removal of alkaline nitride from lubricating oil by modified clays

Mingrong Chen, Naiwang Liu*, Li Shi and Xuan Meng
East China University of Science and Technology, Shanghai 200237, China

Abstract

In order to improve the removal efficiency of clays in oil refining, to explore the related factors and to clarify the removal mechanism of alkaline nitride, a series of modified clays was prepared to test removal of alkaline nitride from lubricating oil. After the addition of 1 wt.% $FeCl_3$, the removal rate of alkaline nitride increased from 33.6% to 43.3%. Furthermore, the acidity and chlorine content did not exceed acceptable levels. The testing methods of N_2 adsorption–desorption, particle-size distribution, Fourier-transform infrared spectroscopy and X-ray diffraction were conducted to verify the removal mechanism. The removal rate of alkaline nitride is mainly related to the density of Lewis acid sites. The Fourier-transform infrared spectra confirmed the existence of the complexation reaction. The basic nitrides were removed by chemical adsorption *via* Fe^{3+}-complexation.

Keywords: adsorption, complexation, denitrogenation, $FeCl_3$, modified clay

(Received 7 October 2021; revised 2 January 2022; Associate Editor: Miroslav Pospíšil)

As one of the quality indexes of oil products, alkaline nitride affects light stability, oxidation stability and additive sensitivity. Under photocatalysis, nitrides can be converted into coloured compounds, which directly affect the colour properties of oil products (Prado *et al.*, 2017). In the presence of a small amount of basic nitride, the solubility of chloride increases, which promotes chloride corrosion in the distillation column, thereby enhancing the corrosion rate compared to in the absence of alkaline nitride, which affects the stability of oil refining and processing (Sagues *et al.*, 1983). In addition, the combination of basic nitrides and acids in oil products may also cause various problems such as pipe blockage and tower corrosion.

At present, the commonly used denitrification processes in major refineries are clay refining and hydrofining (Ho, 1988; Bej *et al.*, 2001; Furimsky & Massoth, 2005; Baia *et al.*, 2017). The former makes use of the strong adsorption capacity of clays and their large specific surface areas to adsorb basic nitrides; this is a low-cost but environmentally unfriendly approach. The latter process can achieve removal by transforming nitride through hydrogenation. However, mild hydrogenation cannot remove most nitrides, and increasing hydrogen pressure means high demand for hydrogen sources and high production costs. Moreover, in hydrofining, hydrodemetallization, hydrodesulfurization, hydrodeoxidization, hydrodearomatization and olefin saturation are all carried out in parallel with hydrodenitrogenation (Raje *et al.*, 1997; Prado *et al.*, 2017), which is not conducive to the denitrification and sulfur retention in lubricating oil. Furthermore, some researchers (Madgavkar & Washecheck, 1988; Qi *et al.*, 1998; Feng, 2004; Hernández-Maldonado & Yang, 2004; Huh *et al.*, 2009; Asumana *et al.*, 2011; Dharaskar Swapnil, 2012; Han *et al.*, 2013; Chen *et al.*, 2014; Martínez-Palou & Luque, 2014; Laredo *et al.*, 2015; Ali *et al.*, 2016; Hizaddin *et al.*, 2016) have proposed processes such as solvent extraction, complex denitrification and the use of ionic liquids, all of which have achieved varying degrees of success.

In general, the liquid–liquid extraction process is achieved in two ways: in the first one, physical extraction is achieved by using the various levels of solubility of basic nitrides in various solvents; and in the second one, the extractant reacts with basic nitrides and selectively dissolves the reaction product to achieve separation. The extraction process is limited by the properties of the solvent, including its boiling point, volatility, solubility, density, polarity, acidity, alkalinity or other chemical properties. Most of the liquid–liquid extraction processes are used in oil products at room temperature, and their denitrification rates are quite different from those of solvents under various conditions. Polar solvents (such as metal salt solutions), acidic solvents, ionic liquids and eutectic solvents have all been proved to be effective extractants, and the latter two have recently become the focus of research because they are environmentally friendly, highly efficient and can be customized (Madgavkar & Washecheck, 1988; Qi *et al.*, 1998; Feng, 2004; Hernández-Maldonado & Yang, 2004; Huh *et al.*, 2009; Asumana *et al.*, 2011; Dharaskar Swapnil, 2012; Han *et al.*, 2013; Chen *et al.*, 2014; Martínez-Palou & Luque, 2014; Laredo *et al.*, 2015; Ali *et al.*, 2016; Hizaddin *et al.*, 2016).

Adsorption is also an important denitrification process, and clays are the most commonly used adsorbents. Adsorption may be either physical or chemical, with the latter usually being more selective but also posing a challenge to the recovery of adsorbents because of the easily modified structures and large specific surface areas of clays, especially in the case of smectites (Fig. 1). In addition to clays, silica gels, ion-exchange resins, activated alumina, zeolites, activated carbon and solid acids have all

*E-mail: liunw@ecust.edu.cn
Cite this article: Chen M, Liu N, Shi L, Meng X (2021). Removal of alkaline nitride from lubricating oil by modified clays. *Clay Minerals* **56**, 261–268. https://doi.org/10.1180/clm.2022.6

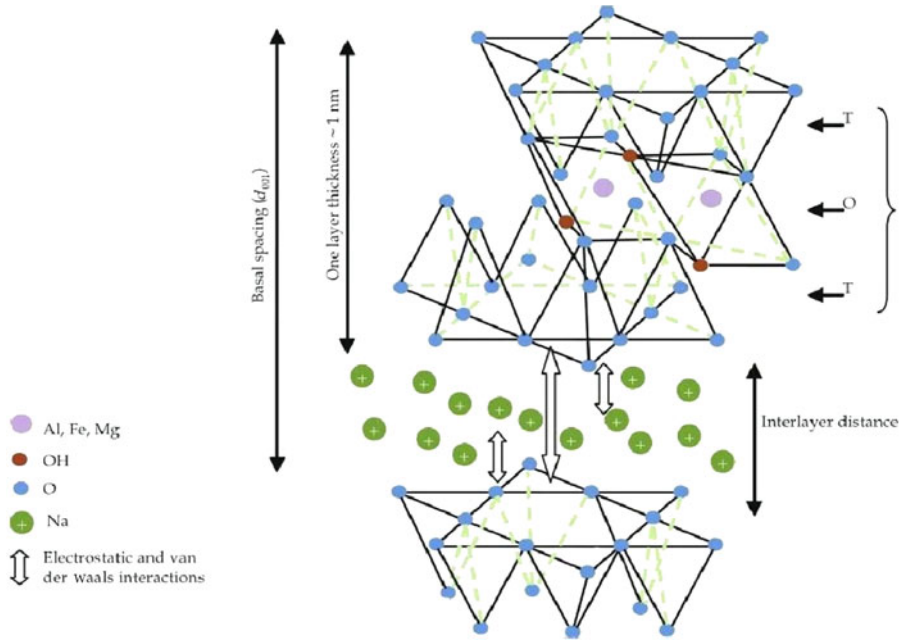

Fig. 1. The structure of smectite clay.

been used for denitrification at lower temperatures (Wang & Li, 2000; Feng, 2004; Sano *et al.*, 2004; Xie *et al.*, 2010; Hong & Tang, 2015).

Clays have not been replaced by the emerging or conventional adsorbents because of their low cost and wide range of applications. Compared with liquid–liquid extraction, the technological process of adsorption and deamination is simpler and the reaction temperature and application conditions are less strict. In addition, the effect of Lewis acids (i.e. metal salts) on the removal of basic nitrides at low temperatures is also significant (Choi & Dines, 1985; Feng, 2004; Zhang *et al.*, 2013).

The denitrification process of the feedstock oil used in this experiment is clay refining at 180°C, with a basic nitride removal rate of ~20–30%. At such a low denitrification rate, the amount of waste clay produced every year is considerable for large refineries, causing tremendous environmental impacts.

This work compares the denitrification efficiency of three bentonitic clays and explores possible factors affecting the process. The bentonites come from various areas and are used as carrier precursors. The physical and chemical properties of the clays were studied. Clay-A, which had best denitrogenation efficiency, was selected, modified with $FeCl_3$ and used to remove basic nitride at 180°C. Our study aims to develop an effective basic nitride adsorbent and to evaluate its removal mechanism.

Experimental

Materials and methods

The raw oil is a vacuum distillation, second-line oil from Sinopec Shanghai Gaoqiao Petrochemical Co., Ltd. (China) with an alkaline nitride content of 56.22 ppm. The three bentonites used are labelled as Clay-A, Clay-B and Clay-C, and they consist mainly of montmorillonite. All bentonites are Ca-rich. Clay-A comes from central China, Clay-B from northern China and Clay-C from north-central China. The bentonites were activated by Baiyue Active Clay Co., Ltd, Anhui (China). The mineralogical and chemical compositions of the clays are shown in Fig. 2 and Table 1. $FeCl_3$, $Fe(NO_3)_3$, C_7H_8 and glacial acetic acid were purchased from Titan Technology Co., Ltd (China).

A total of 50 g of crude oil was added to a three-necked flask with a magnetic rotor and placed in a heating mantle before connecting the electric thermocouple and the N_2 pipeline (Fig. 3). After opening the N_2 valve and adjusting the gas flow, the magnetic rotor began stirring and the reaction temperature was set to 180°C. Adsorbent was added according to mass ratios of agent to oil of 1:50 (clay or modified clay) or 1:100 (pure compound). After 30 min of reaction, the oil was filtered and 10 g of residual crude was weighed for chemical titration.

Clay modification

The three bentonite clays were dried at 150°C for 2 h and ground in a ball mill for 6 h at 300 rpm. Clay-A was further modified with $FeCl_3$ as follows: three aliquots with masses of 0.99, 0.95 and 0.9 g were prepared and 0.01, 0.05 and 0.10 g $FeCl_3$ were added, respectively. This was then dried at 120°C, roasted at 150°C for 2 h and ground to obtain 1 g of Clay-A modified by 1, 5 and 10 wt.% $FeCl_3$, respectively.

Determination of the basic nitride content

The basic nitride content was determined *via* chemical titration using perchloric acid–glacial acetic acid as the titrant and methyl purple as an indicator. The end of titration was marked by the change of the residual oil from purple to blue or from yellow to light green. Measurements were taken in duplicate and the average value of the two results was taken as the final result of denitrification. The differences between the two measurements never exceeded 1 ppm.

N_2 adsorption–desorption characterization

A clean and dry quartz tube was used to record the mass of the empty tube. In total, ~0.1 g of clay powder was loaded into the

https://doi.org/10.1180/clm.2022.6 Published online by Cambridge University Press

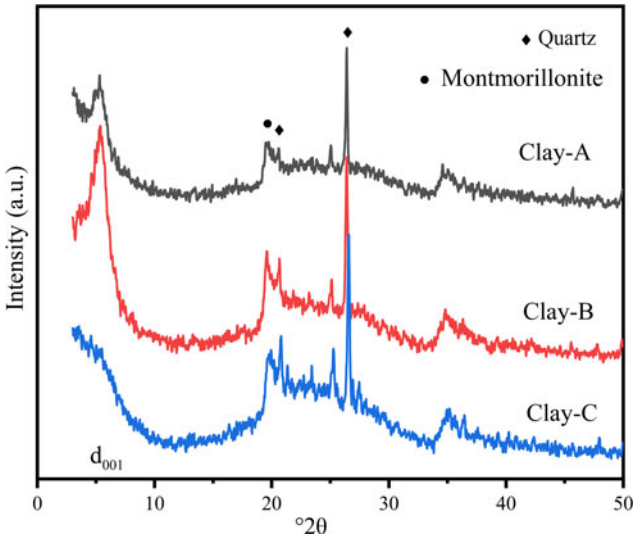

Fig. 2. XRD traces for the carrier clays.

Table 1. Chemical compositions (wt.%) of the bentonite clays.

Oxide	Clay-A	Clay-B	Clay-C
SiO_2	74.2	75.4	76.5
Al_2O_3	14.9	13.9	13.4
Fe_2O_3	3.6	3.4	2.9
MgO	2.7	2.4	2.2
TiO_2	2.2	2.2	2.0
CaO	1.0	1.0	1.2
K_2O	0.5	0.7	0.8
SO_3	0.3	0.5	0.5
P_2O_5	0.2	0.2	0.1
ZrO_2	0.2	0.2	0.2

quartz tube, which was connected to a JWGB ZQ-200C specific surface analyser (Beijing Jingwei Gaobo Co., Ltd, China). The clay was outgassed at 150°C for 3 h in a vacuum and the specific surface area was determined in a liquid nitrogen environment.

Particle-size characterization

A small amount of clay powder was dispersed in deionized water and the particle-size distribution was analysed using an LA960 laser particle size analyser (Horiba Trading Co., Ltd, China).

Fourier-transform infrared spectroscopy

A total of 16.6 mg of dried clay powder was pressed into 13 mm discs under 10 MPa, placed in an *in situ* infrared cell at 10^{-5} Pa at 200°C for 2 h, then cooled to 80°C for 30 min and finally heated again at 200°C for 15 min to induce desorption. The Fourier-transform infrared (FTIR) spectra were obtained as the averages of 32 scans using an IS-10 FTIR spectrometer (Thermo Fisher Scientific, MA, USA).

X-ray diffraction characterization

The mineralogical compositions of the bentonite samples were determined using a Tonda 5000 X-ray diffractometer with Cu-*Kα* radiation (λ = 0.154 nm) at 40 kV, 30 mA, in the range 3–50°2θ, using a curved graphite monochromator. The scanning rate was 0.02°2θ.

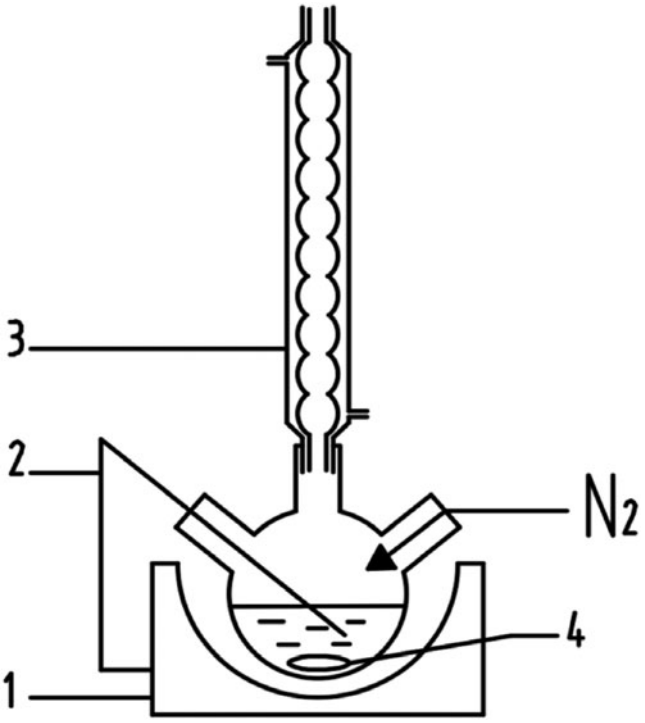

Fig. 3. Schematic diagram of a lubricating oil denitrification unit. 1 = constant-temperature magnetic stirring and heating sleeve; 2 = thermocouple; 3 = condensing tube; 4 = magnetic rotor.

Scanning electron microscopy

The morphology of the smectite particles was determined using scanning electron microscopy (SEM) with an FEI Nova NanoSEM 450 instrument (Thermo Fisher Scientific, MA, USA). Samples were deposited on conductive carbon scotch tape and covered with a gold film 20 nm thick. The SEM images were obtained in the secondary electron mode at a beam energy of 18 keV.

Results and discussion

Influence of the physical and chemical properties of the bentonite clays

Clay-A displayed a good ability to remove alkaline nitride; therefore, it was selected as the carrier clay for further modification (Fig. 4). Based on the difference in alkaline nitride removal capacity of the various clays, we investigated their specific surface data and particle-size distribution data.

There are no direct relationships between the denitrification capacity and the specific surface area, pore volume and pore diameter (Table 2). The adsorption and desorption curves of the three bentonites are all type IV curves, with H4-type hysteresis in the high-relative-pressure section, which is in accordance with the clay structure (Fig. 5). The type IV adsorption isotherm curve indicates initial monolayer adsorption on the mesopore walls followed by capillary condensation when the gas pressure is less than the liquid saturation pressure, forming a liquid phase-like state.

https://doi.org/10.1180/clm.2022.6 Published online by Cambridge University Press

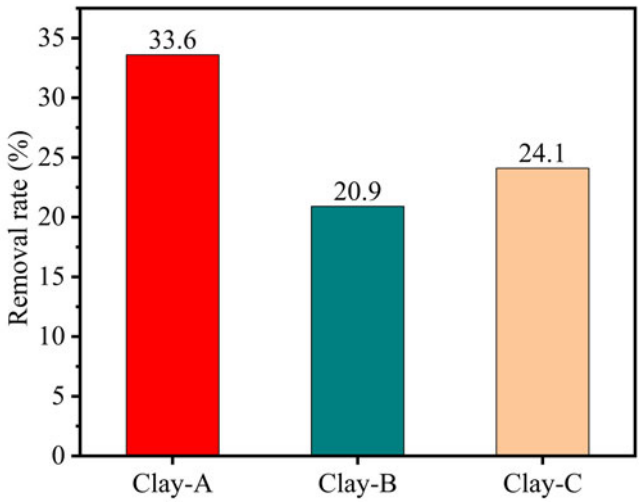

Fig. 4. Alkaline nitride-removal abilities of the bentonite clays. Agent/oil ratio = 1:100, temperature = 180°C, reaction time = 30 min, N_2 atmosphere.

Table 2. Specific surface data of the clays from various ore belts.

Clay	Removal rate	Specific surface area ($m^2\ g^{-1}$)	Pore volume ($cm^3\ g^{-1}$)	Pore size (nm)
Clay-A	33.6%	266	0.3	2.2
Clay-B	20.9%	343	0.4	3.7
Clay-C	24.1%	286	0.3	2.2

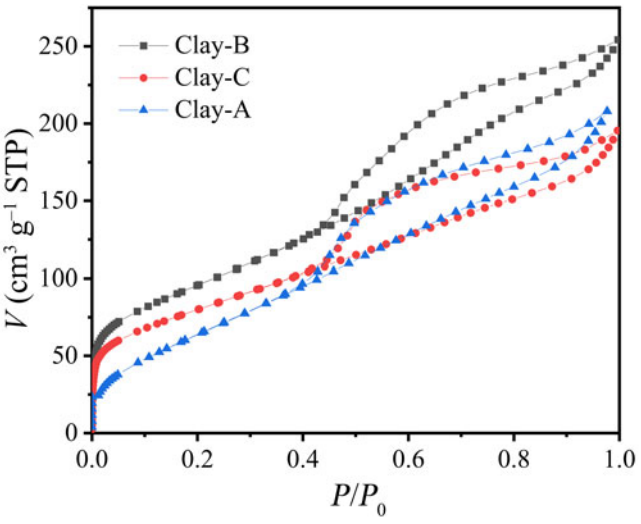

Fig. 5. Isothermal adsorption and desorption curves of the bentonite clays. STP = standard temperature and pressure.

After the capillary condensation fills the mesopore, due to the large pore size or strong interaction with the adsorbate the multimolecular layer adsorption continues to occur and finally forms the adsorption saturation platform. Due to the capillary condensation on the mesopores, the adsorption and desorption curves do not coincide with each other at relative pressures >0.4, resulting in a hysteresis loop. The H4 hysteresis loop means that there is no obvious adsorption platform in the isotherm and that the pore structure of the material is irregular, which is the result of the mixing of pores of various sizes. The three clays displayed similar N_2 adsorption–desorption isotherms (Fig. 5).

Table 3. Particle sizes of the bentonite clays.

Clay	Removal rate	Middle diameter[a] (μm)	Average diameter[b] (μm)	Geometric mean diameter[c] (μm)
Clay-A	33.6%	86.5	133.6	64.1
Clay-B	20.9%	8.9	15.1	9.4
Clay-C	24.1%	108.3	146.1	72.8

[a] The diameter of particles when the transmittance of particles reaches 50% in tests using a laser particle sizer.
[b] The arithmetic mean of the particle-size distribution.
[c] The geometric mean of the particle-size distribution.

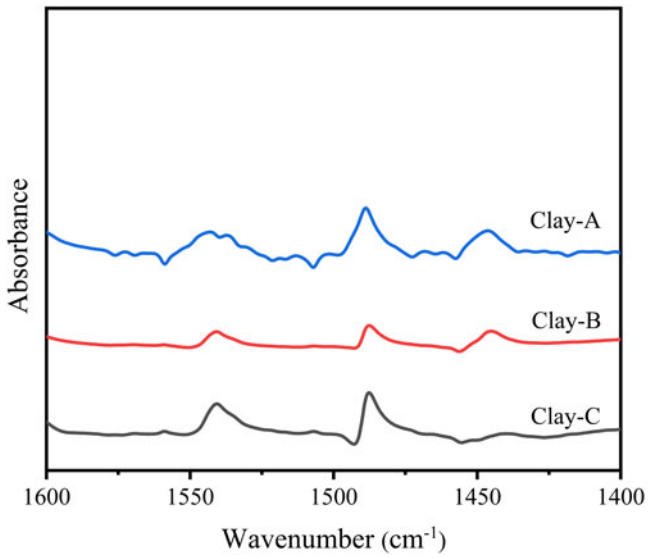

Fig. 6. Surface acidities of the bentonites.

The particle-size data of the clays are listed in Table 3. Clay-A, with its mid-level particle size, has the greatest denitrification capacity (Table 3). Particle size does not affect directly the capacity of the bentonites to remove alkaline nitride.

In summary, the physical structure and properties of the clays have no direct effect on denitrification capacity; hence, the chemical properties were considered. Due to the existence of acid–base neutralization in the denitrification process, the acidities of the clays were investigated.

Both the total acidity and the Lewis acidity seem to improve the clays' ability to remove alkaline nitride (Fig. 6 and Table 4). The relationship between Brønsted acidity and denitrification ability is not clear, however, and we cannot rule out the possibility that a lower Brønsted acidity may also affect denitrification. Previous work (Choi & Dines, 1985; Qi *et al.*, 1998; Zhang *et al.*, 2013) has shown that there are several processes for denitrification using the acid solutions and metal salts as extractants and complexing agents, so the pure Brønsted acid and Lewis acid components were further investigated regarding their ability to remove alkaline nitride at high temperatures.

Influence of ions

Various Brønsted acids (including oxalic acid, citric acid, tartaric acid, ethylenediaminetetraacetic acid, phosphotungstic acid and

https://doi.org/10.1180/clm.2022.6 Published online by Cambridge University Press

Table 4. Surface acidities of the bentonites.

Clay	Removal rate	Total acidity (μmol g^{-1})	Brønsted acidity (μmol g^{-1})	Lewis acidity (μmol g^{-1})
Clay-A	33.6%	66	47	19
Clay-B	20.9%	29	13	15
Clay-C	24.1%	60	54	6

phosphoric acid) and Lewis acids (including ferric chloride, ferrous chloride, zinc chloride, copper chloride, cuprous chloride and aluminium chloride) were used for the removal of basic nitrides, and the results are presented in Fig. 7.

Under the reaction conditions used, oxalic acid and citric acid (Brønsted acids) are unstable and prone to vaporization or decomposition, while $FeCl_3$ and $FeCl_2$ both have excellent ability to remove alkaline nitride (which is difficult to decompose and separate) compared with Brønsted acids.

Previous work has shown that there is an obvious relationship between Lewis acid density and electronegativity: with increasing electronegativity, Lewis acid density increases. Brown & Skowron (1990) summarized two effective correlations between Lewis acid density and electronegativity:

$$\mathrm{Sa} = 1.18\chi^2 \quad \chi = \frac{n_s e_s + n_p e_p}{n_s + n_p} \tag{1}$$

$$\mathrm{Sa} = \frac{V}{N_t} \tag{2}$$

Equation 1 was proposed by Allen (1989). The electronegativity (χ) is calculated using the electron energy correlation constants of the s and p valence layers, and then the Lewis acid density (Sa) of the main-group elements is obtained. Equation 2 was put forward by Brown (1990) after observing the oxidation state (V) and coordination number (N_t) of the ions in a compound. By using the above two formulae, the Sa value of the compound can be obtained and the Lewis acid strength can be compared.

The electronegativity of elements of the same group decreases with increasing atomic number, and the electronegativity of elements of the same period increases with increasing atomic number. For various oxidation states of the same atom, the greater the valence state, the stronger the electronegativity. In general, especially in the main-group elements, electronegativity is consistent with Lewis acid density, although some special cases were pointed out by Brown (1990). The transition elements have comparable electronegativity. Various scales and calculation methods have been proposed to characterize the Lewis acid density, which involve nuclear charges and atomic/ion radii.

The electronegativity of ions as proposed by Li & Xue (2006) includes the sixfold coordination radius (r_i), the limit ionization energy (I_m) and the effective principal quantum number (n^*) of ions, and R = 13.6 eV is the Rydberg constant. I_m is related to the effective charge number and the effective principal quantum number. Based on Equation 1, the Lewis acidity of various ions can be calculated easily from Equation 3.

$$\chi_i = \frac{0.105n^*\left(\frac{I_m}{\mathrm{R}}\right)^{\frac{1}{2}}}{\mathrm{r_i}} + 0.863 \tag{3}$$

Based on the above calculation and analysis, it follows that the Lewis acid density of Fe^{3+} is greater than those of Cu^{2+} and Zn^{2+}, which explains why $FeCl_3$ shows the greatest denitrification effect in various Lewis acids, followed by $FeCl_2$ (Zhang, 1982). Although $AlCl_3$ is the most commonly used high-acidity compound in industry, it is not as effective as $FeCl_3$ in denitrification reactions because it is easy deactivated and lost. In addition, the distribution of valence electrons in the external valence layer of Fe ions provides a more stable environment for binding the lone-pair electrons of basic nitrides, further explaining the excellent denitrification effect of $FeCl_3$.

Based on the high removal rate of Fe^{3+}, the denitrification ability of various iron salts was investigated. Sagues *et al.* (1983) noted that the solubility of chloride increases in the presence of basic

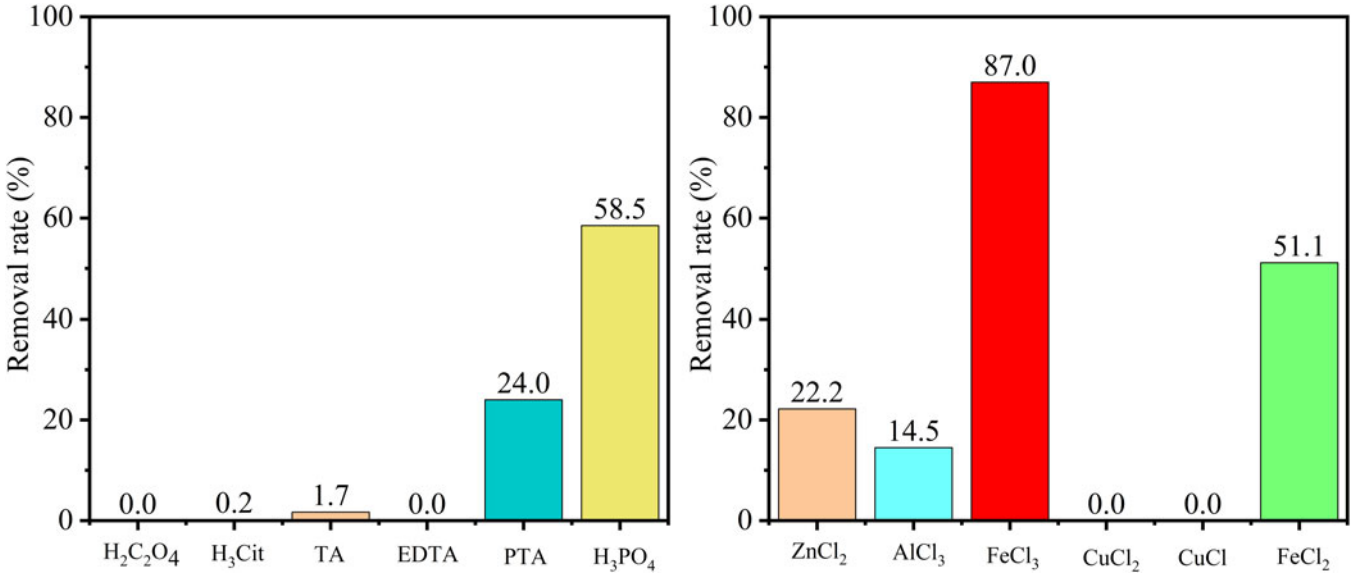

Fig. 7. Removal rates of alkaline nitride by Brønsted acids (left) and Lewis acids (right). Agent/oil ratio = 1:200, temperature = 180°C, reaction time = 30 min, N_2 atmosphere. EDTA = ethylenediaminetetraacetic acid; H_3Cit = citric acid; PTA = phosphotungstic acid; TA = tartaric acid.

https://doi.org/10.1180/clm.2022.6 Published online by Cambridge University Press

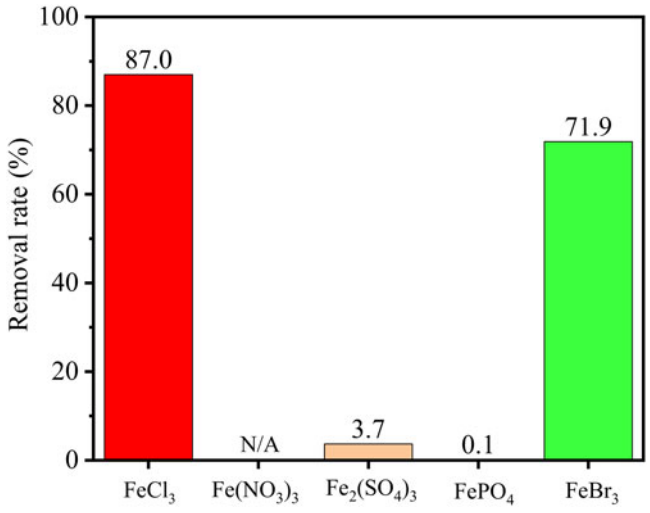

Fig. 8. Denitrification effects of various Fe salts. Agent/oil ratio = 1:200, temperature = 180°C, reaction time = 30 min, N_2 atmosphere.

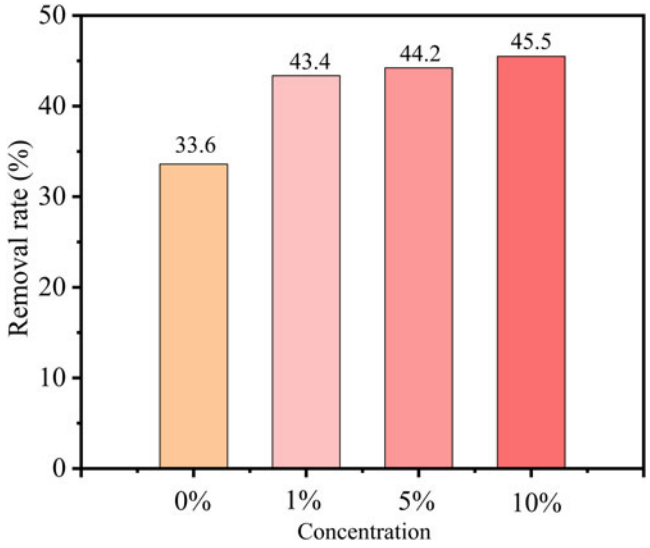

Fig. 9. Denitrification effects of clays under various $FeCl_3$ load concentrations. Agent/oil ratio = 1:100, temperature = 180°C, reaction time = 30 min, N_2 atmosphere.

nitrides, which may pose a potential risk to pipelines and equipment. Because the structure and properties of $FeBr_3$ are similar to $FeCl_3$ but it is slightly less corrosive, the denitrification ability of $FeBr_3$ was also investigated. In addition, because H_3PO_4 also causes denitrification at high temperatures, the role of $FePO_4$ was also considered. Furthermore, due to the principle of the denitrification and sulfur preservation in the processing of lubricating oil, $Fe_2(SO_4)_3$ was also included in this investigation. Finally, $Fe(NO_3)_3$ was used as a supplement to verify the effect of acid ions and nitrogen-containing compounds on the denitrification efficiency of lubricating oil.

The denitrification abilities of $FeCl_3$ and $FeBr_3$ are strong, but the performance of $FeCl_3$ is better at 180°C (Fig. 8). It follows that the factors affecting the denitrification effects of various iron salts are the acidity and basicity of the anions and the ion radius, and this is consistent with the influence of electronegativity mentioned previously and its contribution to Lewis acid density.

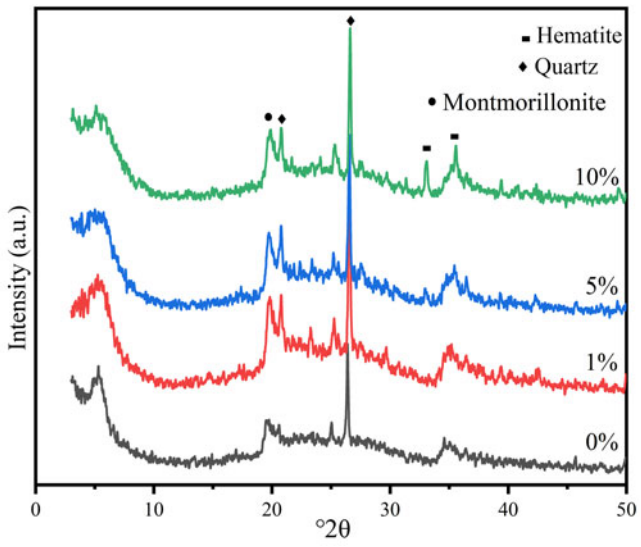

Fig. 10. XRD traces for the clays with various Fe loads.

The alkalinity of NO_3^- is strong, and the residual amount of basic nitride measured at the end of the reaction is greater than that of the raw material. While the ion radii of SO_4^{2-} and PO_4^{3-} are larger than those of Cl^- and Br^-, the electron cloud is widely distributed and the repulsion of nitride lone-pair electrons is strong, leading to a weak electronegativity, which affects the binding of Fe ions and nitrides. On the other hand, the atomic structure and properties of Cl^- and Br^- are similar, but the radius of Cl^- is smaller than that of Br^-, causing greater electronegativity and Lewis acid density in Cl^-; hence, the binding force of nitrides to Fe ions is stronger and the possibility of dissociation at high temperatures is lower, yielding better denitrification. This result is in accordance with the work of Luo & Benson (1991), who showed that the Lewis acid density of Cl was significantly greater than that of Br.

Based on this, $FeCl_3$ was loaded onto Clay-A as an active component and the denitrification effect was investigated. Compared with the carrier clay, the ability to remove alkaline nitride was improved after $FeCl_3$ modification (Fig. 9). However, when increasing the $FeCl_3$ loading beyond 1%, denitrification did not improve further. It is suggested that such a large Fe load caused aggregation of montmorillonite crystals. X-ray diffraction (XRD) traces of Clay-A treated with various amounts of $FeCl_3$ are shown in Fig. 10.

At an $FeCl_3$ load of 1%, no significant changes are observed in the bentonite, suggesting an improved dispersion effect with $FeCl_3$. Hematite formed with increasing $FeCl_3$ loading, and at 10% $FeCl_3$ loading hematite became a major phase. It can be inferred that the dispersion effect is lower in this case than with a low Fe load, causing slow denitrification.

In order to verify the XRD results and the surface species aggregation and morphology changes caused by the increase in $FeCl_3$ load, a SEM analysis was performed, and the results are shown in Fig. 11. When there is no $FeCl_3$ load or at 1% $FeCl_3$ loading, the morphology of the adsorbent tends to be similar and the montmorillonite particles tend to be better dispersed. At $FeCl_3$ loads of 5% or 10%, the surface morphology of the adsorbent changed. Most of the surface of the carrier was covered by $FeCl_3$, which affected the distribution of active species. This explains the fact that a large Fe load does not improve denitrification ability. The SEM images are in accordance with the XRD results.

https://doi.org/10.1180/clm.2022.6 Published online by Cambridge University Press

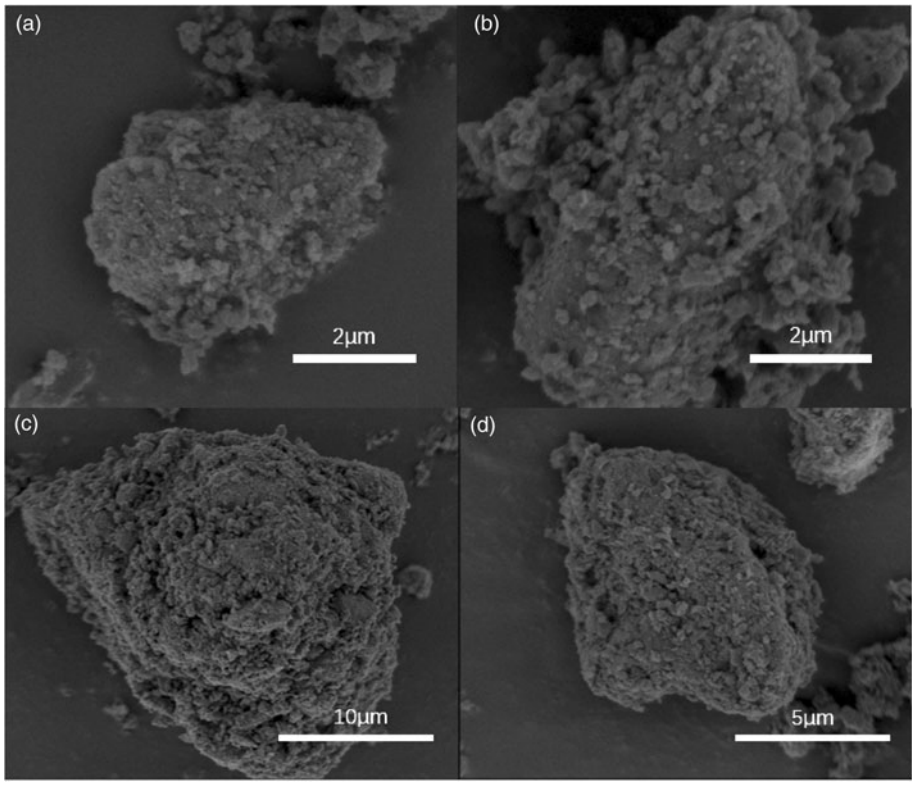

Fig. 11. SEM images of (a) Clay-A, (b) 1% $FeCl_3$/Clay-A, (c) 5% $FeCl_3$/Clay-A and (d) 10% $FeCl_3$/Clay-A.

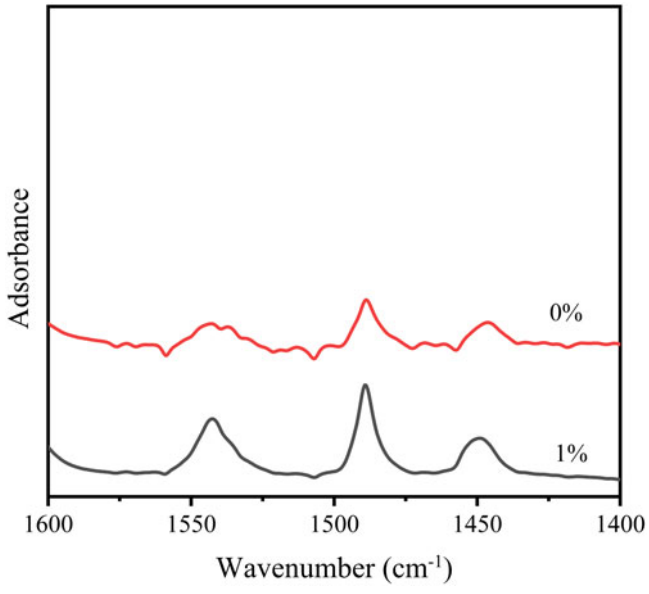

Fig. 12. Surface acidities of Clay-A (0%/1% $FeCl_3$) as assessed from FTIR spectra.

Table 5. Acid content of Clay-A with 0%/1% $FeCl_3$.

$FeCl_3$ concentration	Removal rate	Total acidity (μmol g^{-1})	Brønsted acidity (μmol g^{-1})	Lewis acidity (μmol g^{-1})
0%	33.60%	66	47	19
1%	43.36%	134	92	43

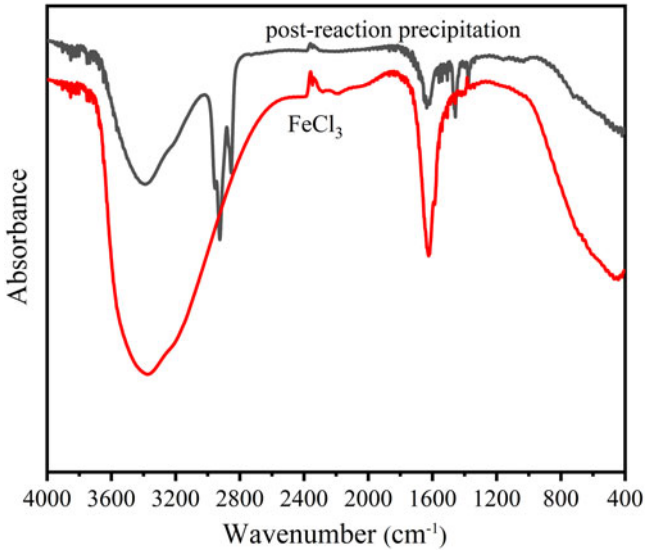

Fig. 13. FTIR spectra of pure $FeCl_3$ and post-reaction precipitation.

The pyridine-FTIR spectra of Clay-A with 1% $FeCl_3$ loading are shown in Fig. 12. Total acidity increases at 1% $FeCl_3$ loading (Table 5). In addition, the acid value and chlorine content of the oil treated with clays loading with 1% $FeCl_3$ did not exceed the maximum acceptable values at 180°C.

Denitrification mechanism

The pure $FeCl_3$ and post-reaction precipitation were examined using FTIR spectroscopy with the KBr technique. New bands

https://doi.org/10.1180/clm.2022.6 Published online by Cambridge University Press

appeared in the 3000–2800 and 1500–1300 cm^{-1} regions of the complex product compared with $FeCl_3$ (Fig. 13). The bands at 3070 and 3020 cm^{-1} are attributed to C–H stretching in pyridine and that at 3030 cm^{-1} is attributed to quinoline and aniline. By comparing the spectra before and after the reaction with the spectra of basic nitrides, a red shift can be seen, as the C–H band of basic nitrides shifts from 3100–3000 to 3000–2900 cm^{-1}. It is suggested that when Fe^{3+} adsorbs basic nitrides, it coordinates with them, and this coordination would occur according to Equation 4:

$$FeCl_3 + nRN \leftrightarrow [Fe\text{-}nRN]Cl_m \quad (4)$$

where n and m refer to any number of the basic nitrides and Cl^- that take part in the complexation reaction and R refers to the alkyl of the basic nitrides.

Conclusion

A Chinese bentonite showing good denitrification performance was selected as a carrier for oil denitrification treatment and 1% $FeCl_3$ was added to modify the clay. Under the reaction conditions, the denitrification rate increased from 33.6% to 43.4%. Through characterization and analysis of the clay, some conclusions can be inferred:

(1) The physical structure of the clay does not affect denitrification performance. Nevertheless, the acid content of the clay influences denitrification performance.
(2) Compared with Brønsted acids, Lewis acids are superior for removing alkaline nitride, and $FeCl_3$ is efficient under the specific reaction conditions used in this study.
(3) The vibration bands of basic nitrides red-shifted from 3100–3000 to 3000–2900 cm^{-1}, indicating a strong combination between basic nitrogen and Fe^{3+}, with the binding mode being complex.

In a subsequent experiment, the specific species of basic nitrides in lubricating oil and the various adsorptions of specific nitrogen species by $FeCl_3$ will be considered.

Financial support. This work was supported by the National Natural Science Foundation of China (No. 21808054).

References

Ali M.C., Yang Q., Fine A.A., Jin W., Zhang Z., Xing H. & Ren Q. (2016) Efficient removal of both basic and non-basic nitrogen compounds from fuels by deep eutectic solvents. *Green Chemistry*, **18**, 157–164.

Allen L.C. (1989) Electronegativity is the average one-electron energy of the valence-shell electrons in ground-state free atoms. *Journal of the American Chemical Society*, **111**, 9003–9014.

Asumana C., Yu G., Guan Y., Yang S., Zhou S. & Chen X. (2011) Extractive denitrogenation of fuel oils with dicyanamide-based ionic liquids. *Green Chemistry*, **13**, 3300–3305.

Baia L.V., Souza W.C., de Souza R.J.F., Veloso C.O., Chiaro S.S.X. & Figueiredo M.A.G. (2017) Removal of sulfur and nitrogen compounds from diesel oil by adsorption using clays as adsorbents. *Energy & Fuels*, **31**, 11731–11742.

Bej S.K., Dalai A.K. & Adjaye J. (2001) Comparison of hydrodenitrogenation of basic and nonbasic nitrogen compounds present in oil sands derived heavy gas oil. *Energy & Fuels*, **15**, 377–383.

Brown I. & Skowron A. (1990) Electronegativity and Lewis acid strength. *Journal of the American Chemical Society*, **112**, 3401–3403.

Chen X., Yuan S., Abdeltawab A.A., Al-Deyab S.S., Zhang J., Yu L. & Yu G. (2014) Extractive desulfurization and denitrogenation of fuels using functional acidic ionic liquids. *Separation and Purification Technology*, **133**, 187–193.

Choi H.W. & Dines M.B. (1985) Selective removal of nitrogen compounds from shale oil. *Fuel*, **64**, 4–8.

Dharaskar Swapnil A. (2012) Ionic liquids (a review): the green solvents for petroleum and hydrocarbon industries. *Research Journal of Chemical Sciences ISSN*, **2**, 80–85.

Feng Y. (2004) A study on the process conditions of removing basic nitrogen compounds from gasoline. *Petroleum Science and Technology*, **22**, 1517–1525.

Furimsky E. & Massoth F.E. (2005) Hydrodenitrogenation of petroleum. *Catalysis Reviews*, **47**, 297–489.

Han D., Li G., Cao Z., Zhai X. & Yuan M. (2013) A study on the denitrogenation of Fushun shale oil. *Energy Sources, Part A: Recovery, Utilization, and Environmental Effects*, **35**, 622–628.

Hernández-Maldonado A.J. & Yang R.T. (2004) Denitrogenation of transportation fuels by zeolites at ambient temperature and pressure. *Angewandte Chemie*, **116**, 1022–1024.

Hizaddin H.F., Hadj-Kali M.K., Ramalingam A. & Hashim M.A. (2016) Extractive denitrogenation of diesel fuel using ammonium-and phosphonium-based deep eutectic solvents. *Journal of Chemical Thermodynamics*, **95**, 164–173.

Ho T.C. (1988) Hydrodenitrogenation catalysis. *Catalysis Reviews Science and Engineering*, **30**, 117–160.

Hong X. & Tang K. (2015) Absorptive denitrogenation of diesel oil using a modified nay molecular sieve. *Petroleum Science and Technology*, **33**, 1471–1478.

Huh E.S., Zazybin A., Palgunadi J., Ahn S., Hong J., Kim H.S. *et al.* (2009) Zn-containing ionic liquids for the extractive denitrogenation of a model oil: a mechanistic consideration. *Energy & Fuels*, **23**, 3032–3038.

Laredo G.C., Likhanova N.V., Lijanova I.V., Rodriguez-Heredia B., Castillo J.J. & Perez-Romo P. (2015) Synthesis of ionic liquids and their use for extracting nitrogen compounds from gas oil feeds towards diesel fuel production. *Fuel Processing Technology*, **130**, 38–45.

Li K. & Xue D. (2006) Estimation of electronegativity values of elements in different valence states. *Journal of Physical Chemistry A*, **110**, 11332–11337.

Luo Y.R. & Benson S.W. (1991) A new electronegativity scale. 12. Intrinsic Lewis acid strength for main-group elements. *Inorganic Chemistry*, **30**, 1676–1677.

Madgavkar A.M. & Washecheck D.M. (1988) *Two-Step Heterocyclic Nitrogen Extraction from Petroleum Oils*. US 4671865A.

Martínez-Palou R. & Luque R. (2014) Applications of ionic liquids in the removal of contaminants from refinery feedstocks: an industrial perspective. *Energy & Environmental Science*, **7**, 2414–2447.

Prado G.H.C., Rao Y. & de Klerk A. (2017) Nitrogen removal from oil: a review. *Energy & Fuels*, **31**, 14–36.

Qi J., Yan Y., Su Y., Qu F. & Dai Y. (1998) Extraction of nitrogen compounds from catalytically cracked diesel oil with a volatile carboxylic acid based on reversible chemical complexation. *Energy & Fuels*, **12**, 788–791.

Raje A.P., Liaw S.-J., Srinivasan R. & Davis B.H. (1997) Second row transition metal sulfides for the hydrotreatment of coal-derived naphtha I. Catalyst preparation, characterization and comparison of rate of simultaneous removal of total sulfur, nitrogen and oxygen. *Applied Catalysis A: General*, **150**, 297–318.

Sagues A.A., Davis B.H. & Johnson T. (1983) Coal liquids distillation tower corrosion. Synergistic effects of chlorides, phenols, and basic nitrogen compounds. *Industrial & Engineering Chemistry Process Design and Development*, **22**, 15–22.

Sano Y., Choi K.-H., Korai Y. & Mochida I. (2004) Adsorptive removal of sulfur and nitrogen species from a straight run gas oil over activated carbons for its deep hydrodesulfurization. *Applied Catalysis B: Environmental*, **49**, 219–225.

Wang Y. & Li R. (2000) Denitrogenation of lubricating base oils by solid acid. *Petroleum Science and Technology*, **18**, 965–973.

Xie L.-L., Favre-Reguillon A., Wang X.-X., Fu X. & Lemaire M. (2010) Selective adsorption of neutral nitrogen compounds from fuel using ion-exchange resins. *Journal of Chemical & Engineering Data*, **55**, 4849–4853.

Zhang J., Xu J., Qian J. & Liu L. (2013) Denitrogenation of straight-run diesel with complexing extraction. *Petroleum Science and Technology*, **31**, 777–782.

Zhang Y. (1982) Electronegativities of elements in valence states and their applications. 2. A scale for strengths of Lewis acids. *Inorganic Chemistry*, **21**, 3889–3893.

https://doi.org/10.1180/clm.2022.6 Published online by Cambridge University Press